CARES Theory Guide

CERAMICS ANALYSIS AND RELIABILITY EVALUATION OF STRUCTURES

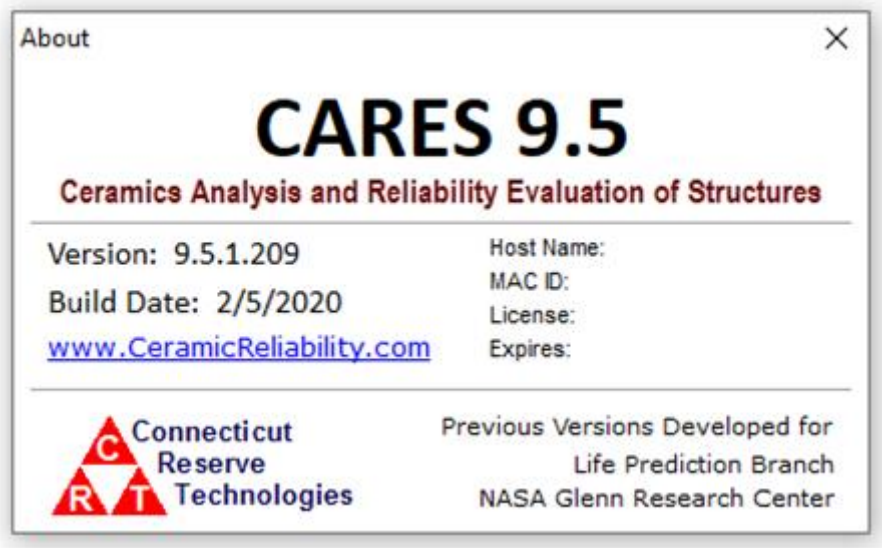

Copyright © Connecticut Reserve Technologies, Inc. February 08, 2020

INTRODUCTION

The following sections of the CARES theory guide will present fundamental concepts and models associated with performing time-independent and time-dependent reliability analyses. The effort to develop CARES has its roots in the application of ceramic components in turbine engines, e.g., stator vanes, rotors, nozzles and combustor liners [1-11]. However, the discussion contained within this guide is not limited to materials exposed to elevated service temperatures. The concepts are easily extended to more mundane applications where brittle materials such as glass or cements are utilized. Specific applications that have utilized ceramic materials at near ambient temperatures include wear parts (nozzles, valves, seals, etc.), cutting tools, grinding wheels, bearings, coatings, electronics, and human prostheses. Other brittle materials, such as glass and graphite materials have been used in the fabrication of infrared transmission windows, glass skyscraper panels, television cathode ray tubes, and high-temperature graphite bearings. The design methodologies used to analyze these types of components, as well as components exposed to elevated service temperatures, are presented in this guide.

From a design engineer's perspective, brittle materials such as ceramics often exhibit attractive high strength properties at service temperatures that are well beyond use temperatures of conventional ductile materials. For advanced diesel and turbine engines, ceramic components have already demonstrated functional abilities at temperatures reaching 1371 °C, which is well beyond the operational limits of most conventional metal alloys. However, a penalty is paid in that these materials typically exhibit low fracture toughness, which is usually defined by a critical stress intensity factor, and typically quantified by K_{IC}. This combination of high strength and low fracture toughness leads to a lack of ductility (i.e., lack of fracture toughness) which results in low strain tolerance and large variations in observed fracture strength.

Accounting for the inherent scatter in strength requires a change in philosophy on the design engineer's part that leads to a reduced focus on the use of safety factors in favor of reliability analyses. If a brittle material with an obvious scatter in tensile strength is selected for its high strength attributes, or inert behavior, then components should be designed using an appropriate design methodology rooted in statistical analysis. The reliability approach presented here demands that the design engineer must tolerate a finite risk of unacceptable performance. This risk of unacceptable performance is identified as a component's probability of failure (or alternatively, component reliability). The primary concern of the engineer is minimizing this risk in an economical manner. The contents of this theory guide will clearly outline the concepts that support the software algorithms associated with this guide.

PROBABILISTIC APPROACH TO DESIGN

An engineer is trained to quantify component failure through the use of a safety factor. By definition, the safety factor for a component subjected to a single load L is given by the ratio

$$Safety\ Factor = \frac{R}{L} \tag{1}$$

where R is the resistance (or strength) of the material from which the component is fabricated. Making use of the concept of a safety factor, the probability of failure (P_f) for the component where a single load is applied is given by the expression

$$P_f = Probability\left(\frac{R}{L} \geq 1\right) \tag{2}$$

In making the transition from a deterministic safety factor for a component to a probability of failure, for the most general case, the assumption is made that both R and L are random variables. Under this assumption P_f is the product of two finite probabilities summed over all possible outcomes. Both probabilities are associated with an event and a random variable.

The first event is defined by the random variable L taking on a value in the range

$$\left(x - \frac{dx}{2}\right) \leq L \leq \left(x + \frac{dx}{2}\right) \tag{3}$$

The probability associated with this event is the area under the probability density function (PDF) for the load random variable (f_L) over this interval, i.e.,

$$P_1 = f_L(x)\,dx \tag{4}$$

The second event is associated with the probability that the random variable R is less than or equal to x. This is the area under the probability density for the resistance random variable (f_R) from minus infinity (or an appropriate lower limit defined by the range of the resistance random variable) to x. This second probability is given by the cumulative distribution function (CDF) for the resistance random variable (F_R) evaluated at x, i.e.,

$$P_2 = F_R(x) \tag{5}$$

With the probability of failure defined as the product of these two probabilities, summed over all possible values of x, then

$$\begin{aligned} P_f &= P_1 P_2 \\ &= \int_{-\infty}^{+\infty} F_R(x)\, f_L(x)dx \end{aligned} \tag{6}$$

To interpret this integral expression, consider the graphs in Fig 1. In this figure, the graph of an arbitrary probability density function for the resistance random variable is superimposed on the graph of an arbitrary probability density function for the load random variable. Note that *R* and *L* must have the same dimensional units (e.g., force or stress) to superimpose their graphs in the same figure. A common misconception is that P_f is the area of overlap encompassed by the two probability density functions. Scrutiny of equation 6 leads to the appropriate conclusion that the probability of failure is really the area under the composite function

$$g_{RL}(x) = F_R(x)\ f_L(x) \qquad \textbf{(7)}$$

which is also illustrated in Figure 1.

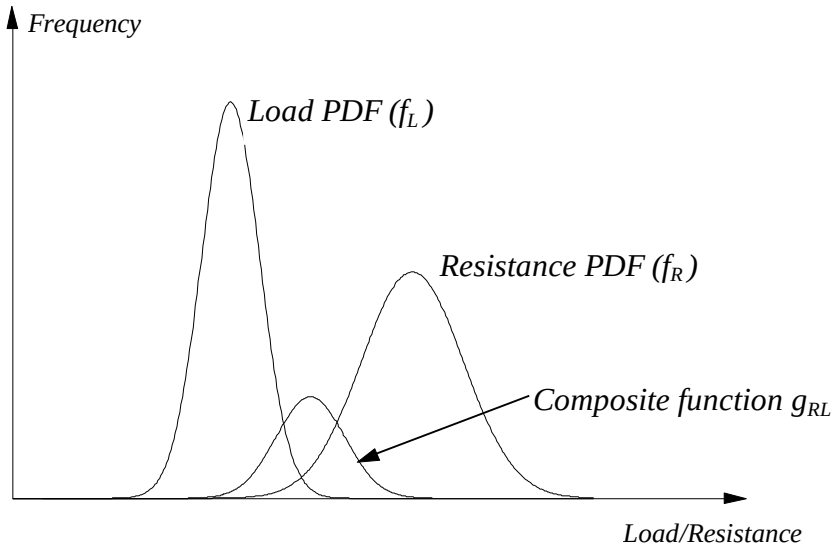

Figure 1 Interference Plot for Load and Resistance Random Variables

Next, consider the situation where the load random variable has very little scatter relative to the resistance random variable. For example, if a number of test specimens were fabricated from a brittle material, say for instance a monolithic ceramic, the ultimate tensile strength can easily vary by over 100%. That is, the highest strength value in the group tested can easily be twice as large as the lowest value. Variations of this magnitude are not typical for the load design variable, and the engineer could easily conclude that load is a deterministic design variable while strength is a random design variable. This assumption can be accommodated in this development by allowing the probability density function for the load random variable to be defined by the expression

$$f_L(x) = \delta(x - x_o) \qquad \textbf{(8)}$$

Here δ is the Dirac delta function defined as

$$\delta(x - x_o) = \begin{cases} \infty & x = x_o \\ 0 & x \neq x_o \end{cases} \quad \textbf{(9)}$$

Note that the Dirac delta function satisfies the definition for a probability density function, i.e., the area under the curve is equal to one, and the function is greater than or equal to zero for all values of x. The Dirac delta function represents the scenario where the standard deviation of a random variable approaches zero in the limit, and the random variable takes on a single value, i.e., the central value identified here as x_o.

Since the Dirac delta function is being used to represent the load random variable, then x_o really represents the deterministic magnitude of the applied load. Keep in mind that the applied load can have units of force or stress. However, load and resistance are commonly represented with units of stress. Thus x_o is replaced with σ, an applied stress, and the probability of failure is given by the expression

$$P_f = \int_{-\infty}^{+\infty} F_R(x)\delta(x - \sigma)dx \quad \textbf{(10)}$$

However, with the Dirac delta function embedded in the integral expression, the probability of failure simplifies to

$$P_f = F_R(\sigma) \quad \textbf{(11)}$$

Thus the probability of failure is equal to the CDF of the resistance random variable evaluated at the applied load, σ. The use of the Dirac delta function in representing the load design variable provides justification for the use of the Weibull CDF (or a similarly skewed distribution) in quantifying the probability of failure for components fabricated from ceramics or glass.

The motivation for equation 11, which appears throughout the ceramics and glass literature, has been provided. The next step is the extension of this expression to components with multiaxial states of stress.

TIME-INDEPENDENT WEIBULL ANALYSIS (FAST FRACTURE)

Reliability analyses are typically segregated into two categories: time-independent (also referred to as fast fracture) and time-dependent. This classification is rooted both in the historic development of the reliability models presented here and also in a practical approach to the analysis of a component. In many instances, a component must perform in an adequate fashion over a predetermined service life. To accomplish this design goal, the component must survive the initial load cycle. Thus the calculated time-independent reliability value is used as a screening criterion, and is also used as an initial value for the time-dependent analyses discussed later. A fundamental premise of probabilistic analysis dictates that if the reliability of a component varies with time then it should never exceed the fast fracture reliability value (unless there exists some physical mechanism such as flaw healing that can account for this phenomenon). From a historical perspective time-independent models were developed first (hence they are presented here first).

Fracture Mechanics vs. Weibull Analysis

When metal components are subjected to applied loads the material has the capacity to generate dislocations that migrate through the microstructure. This property permits yielding and minor shape adjustments without catastrophic failure of the component. Structural ceramics and other brittle materials typically do not have this property and therefore their failure behavior is very brittle in comparison to metals. As a result ceramic components are highly sensitive to stress concentrations, microstructural inhomogeneities, surface damage from processing, and/or dimensional tolerances that are not met. This brittle behavior would seemingly point to the use of fracture mechanics in conducting failure analyses of components. However, there are drawbacks that must be considered.

Fracture mechanics is based on the assumption that failure takes place due to the presence of a defect in the microstructure. The approach describes the stress distribution in the near vicinity of the sharp (or blunt) leading edge of a defect, which results in expressions that indicate the existence of a stress singularity at the tip of the defect. Nearly all singularity expressions involve a ($1/\sqrt{r}$) term, where r is a radial distance from the crack tip. As r approaches zero, stresses become infinite. Since materials cannot sustain an applied stress that goes to infinity, the material fails near the crack tip and the defect advances through material. The advancing crack will move in a stable or unstable fashion depending on the material, applied load and geometry of the component.

The failure process just described is typically quantified through the use of a stress intensity factor (K), although one can appeal to the use of strain energy release rates (G) as well. The stress intensity factor defines the stress amplitude of the crack tip singularity, i.e., stresses in the singularity zone increase in proportion to K. Moreover, the stress intensity factor completely defines the crack tip condition. If K is known, then it is possible to determine all components of stress, strain and displacement. There are numerous stress intensity expressions that are functions of component geometry, far-field stress and a characteristic size of the defect. A component geometry factor, the applied far-field stress, and the current crack length can characterize most stress intensity relationships. When a critical combination of stress and crack length produces failure for a given component geometry, the critical stress intensity level (Kc) is

attained. This value is a material property and is referred to as the fracture toughness of the material.

The stress intensity relationship can be used to design components in one of two ways:

- fracture toughness is specified *a priori* – materials are screened based on this value, and
- the material is pre-selected – critical combinations of applied stress and defect length are determined.

If ceramic materials are utilized to fabricate structural components, then component design falls under the second category. If fracture mechanics is used, then design engineers must determine critical combinations of applied far-field stress, defect length and defect orientation whereby the performance of the structural component would be deemed unacceptable. Here the design procedure based on fracture mechanics reduces to determining the defect length and orientation that will provide acceptable margins under applied loads. In practical terms this means characterizing a critical flaw, i.e., size and orientation. Once this characterization has taken place, all components must be inspected in a non-destructive fashion to determine the presence of this critical flaw. If the flaw is detected, then the component is removed from service. The design process just described seems simple at first; however, for ceramic materials complications arise. ***On relative terms, a material with high strength and low fracture toughness typically has critical flaw sizes that are quite small. These small defects can easily go undetected during inspection procedures.***

Thus, the component fabricated from ceramic materials will contain a distribution of defects with variable lengths and orientations even if the material is inspected using the best available non-destructive evaluation (NDE) methods. Under this condition, performing strength tests makes fundamental sense and attempting to pursue a fracture mechanics approach is not a worthwhile endeavor. A distribution of flaw sizes as well as orientations is present in a ceramic material, and the strength test will exploit the critical flaw. ***Since the critical flaw length and orientation will vary from sample to sample, a distribution in strength is expected.*** From a component standpoint, if the size and orientation of the critical flaw are random, then the critical flaw causing failure may not be located in the region of a component subjected to the maximum applied stress. As a result the stress field throughout the entire component must be analyzed and this information must be combined with the statistical nature of the defects distributed throughout the component. Weibull analysis is well suited to this task.

Accounting for Size Effects: System Reliability

A rather unique property of most brittle materials with high tensile strength and low fracture toughness is an apparent decrease in tensile strength as the size of the component increases. This is the so-called strength-size effect and is a direct result of the distribution of flaws present in the material. An illustration of strength-size-scaling is shown in Figure 2 for a variety of uniaxial and biaxial flexure tests on a 96%-pure alumina [12]. Design methods for ceramic components must admit size dependence. This is accomplished through the use of

system reliability concepts where the component is treated as a system, and the probability of failure of the system must be ascertained.

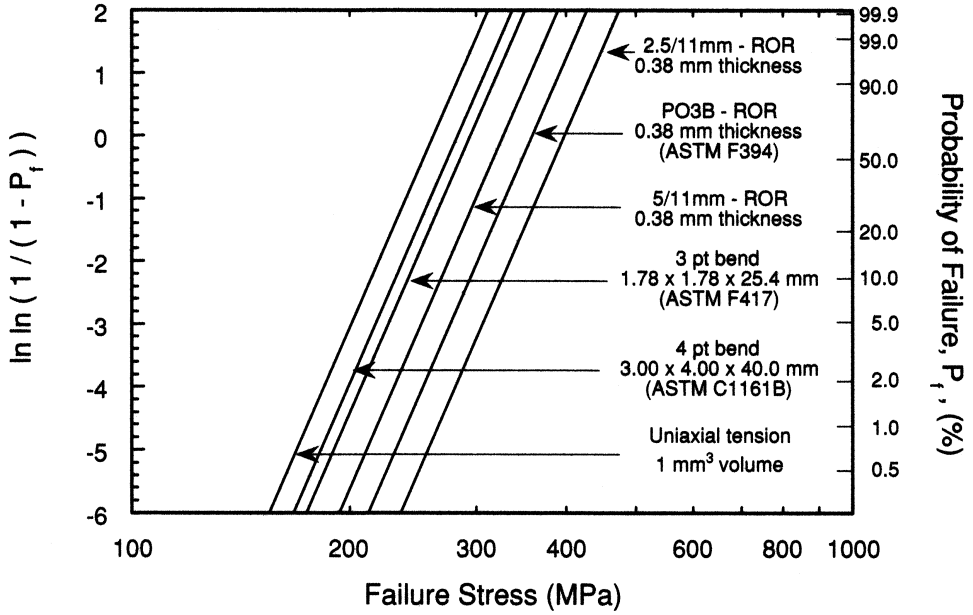

Figure 2 Example of Strength-Size-Scaling in an Alumina Ceramic. Smaller Effective Sizes Result in Higher Failure Stresses [12]

The typical approach to designing structural components with varying stress fields involves discretizing the component in order to characterize the stress field using finite element methods. Since component failure may initiate in any of the discrete elements, it is convenient to consider a component as a system and utilize system reliability theories. A component is a series system if it fails when one discrete element fails. This type of failure can be modeled using weakest-link reliability theories. A component is a parallel system when failure of a single element does not cause the component to fail. In this latter case, the remaining elements sustain load through redistribution. This type of failure can be modeled with what has been referred to in the literature as "bundle theories." Weakest-link theories and bundle theories represent the extremes of failure behavior modeled by reliability analysis. They suggest more complex systems such as *"r out of n"* systems. Here a component (system) of n elements functions if at least r elements have not failed. This type of system model has not found widespread application in structural reliability analysis. The historical perspective has been to assume that the failure behavior of the brittle materials is sudden and catastrophic. This type of behavior fits within the description of a series system, thus a weakest-link reliability system is adopted.

Now the probability of failure of a discrete element must be related to the overall probability of failure of the component. If the failure of an individual element is considered a statistical event, and if these events are independent, then the probability of failure of a discretized component that acts as a series system is given by the expression

$$P_f = 1 - \prod_{i=1}^{N}(1 - \mathrm{P}_i) \quad \textbf{(12)}$$

where N is the number of finite elements for a given component analysis. Here $\mathrm{P_i}$ is the probability of failure of the i^{th} discrete element. The next step involves adopting an expression for the probability of failure (or alternatively, the reliability) of the i^{th} discrete element for a simplified state of stress, i.e., a uniaxial tensile stress. In the ceramic and glass industry the Weibull distribution [13,14] is universally accepted as the distribution of choice in representing the underlying probability distribution function for tensile strength. A two-parameter formulation and a three-parameter formulation are available for the Weibull distribution. However, the two-parameter formulation usually leads to a more conservative estimate for the component probability of failure. The two-parameter Weibull probability density function for a continuous random strength variable, denoted as Σ, is given by the expression

$$f_\Sigma(\sigma) = \left(\frac{\alpha}{\beta}\right)\left(\frac{\sigma}{\beta}\right)^{(\alpha-1)} exp\left[-\left(\frac{\sigma}{\beta}\right)^{\alpha}\right] \quad \textbf{(13)}$$

for $\sigma > 0$, and

$$f_\Sigma(\sigma) = 0 \quad \textbf{(14)}$$

for $\sigma \leq 0$. The cumulative distribution is given by the expression

$$F_\Sigma(\sigma) = 1 - exp\left[-\left(\frac{\sigma}{\beta}\right)^{\alpha}\right] \quad \textbf{(15)}$$

for $\sigma > 0$ and

$$F_\Sigma(\sigma) = 0 \quad \textbf{(16)}$$

for $\sigma \leq 0$. Here α (a scatter parameter, or Weibull modulus) and β (a central location parameter, or typically referred to as the Weibull scale parameter) are distribution parameters. In the ceramic literature when the two-parameter Weibull formulation is adopted then "m" is used for the Weibull modulus α, and "σ_0" or "σ_θ" is used for the Weibull central location parameter. A thorough description of established means for reporting Weibull distribution parameters can be found in American Society for Testing and Materials (ASTM) C1239 [15]. Thus if the random variable representing uniaxial tensile strength of an advanced ceramic is characterized by a two-parameter Weibull distribution, then the probability that a uniaxial test specimen fabricated from an advanced ceramic will fail can be expressed by the cumulative distribution function

$$P_f = 1 - exp\left[-\left(\frac{\sigma_{max}}{\sigma_\theta}\right)^{m}\right] \quad \textbf{(17)}$$

Note that σ_{max} is the maximum normal stress in the component. When used in the context of characterizing the strength of ceramics and glasses, the central location parameter is referred to as the Weibull characteristic strength (σ_θ). The characteristic strength is dependent on the uniaxial test specimen (tensile, flexural, pressurized ring, etc.) used to generate the failure data. For a given material, this parameter will change in magnitude with specimen geometry (the so-called size effect alluded to earlier). The Weibull characteristic strength has units of stress and is not a material parameter as it is a function of geometry and the nature of the applied tensile stress. The scatter parameter *m* is dimensionless.

With the tensile strength characterized by the two-parameter Weibull distribution the discussion returns to the weakest link expression for component probability of failure. Let $\Re_i$ represent the reliability of the i^{th} discrete element where

$$\Re_i = 1 - P_i \tag{18}$$

The reliability of this discrete element is then governed by the following expression

$$\Re_i = exp\left(-\left(\frac{\sigma}{\sigma_0} \right)^m \Delta V \right) \tag{19}$$

where σ is the principal tensile stress applied to the discrete element, and ΔV identifies the volume of this arbitrary discrete element. In this expression, σ_0 is the Weibull material scale parameter and can be described as the Weibull characteristic strength of a specimen with unit volume loaded in uniform uniaxial tension. This is a material-specific parameter that is utilized in the component reliability analyses that follow. The dimensions of this parameter are based on the dimensional field in question and are: stress × (volume)$^{1/m}$ when volume flaws are the strength limiter; stress × (area)$^{1/m}$ when surface flaws are the strength limiter; and stress × (edge length)$^{1/m}$ when edge flaws are the strength limiter. Note - the use of established fractographic practices [16] allow the researcher to censor each i^{th} strength value with respect to the dimensional field of the strength-limiting flaw.

Under the assumptions that the component consists of an infinite number of elements (i.e., the continuum assumption), considering an example when volume flaws are the strength limiter, and that the component is best represented by a series system, then

$$P_f = 1 - \lim_{k \to \infty} \left(\prod_{i=1}^{k} \Re_i \right) \tag{20}$$

Substituting for $\Re_i$ yields

$$P_f = 1 - exp\left(- \lim_{k\to\infty} \sum_{i=1}^{k} \left(\left(\frac{\sigma}{\sigma_0} \right)^m \Delta V \right)_i \right) \quad \textbf{(21)}$$

Here ΔV once again represents the volume of an element. The limit inside the bracket is a Riemann sum, thus

$$P_f = 1 - exp\left[-\int \left(\frac{\sigma}{\sigma_0} \right)^m dV \right] \quad \textbf{(22)}$$

Weibull [13] first proposed this integral representation for the probability of failure. The expression is integrated over all tensile regions of the specimen volume if the strength-controlling flaws are randomly distributed through the volume of the material, or over all tensile regions of the specimen area if flaws are restricted to the specimen surface. For failures due to surface defects the probability of failure is given by the expression

$$P_f = 1 - exp\left[-\int \left(\frac{\sigma}{\sigma_0} \right)^m dA \right] \quad \textbf{(23)}$$

Equations 22 and 23 have historically served as the starting point for reliability analyses of components fabricated from ceramic materials. Note that an analogous expression to relate P_f to σ when edge flaws are the strength limiter can in turn be defined as

$$P_f = 1 - \exp\left[-\int \left(\frac{\sigma}{\sigma_0} \right)^m dL \right] \quad \textbf{(24)}$$

Component reliability analyses presented elsewhere representing different schools of thought from around the world find their genesis in these expressions.

Multiaxial Reliability Models

Over the years a number of reliability models have been presented that extend the uniaxial format of equation 22 through equation 24 to multiaxial states of stress. Only models associated with isotropic brittle materials are available in the CARES algorithm. Anisotropic reliability models are beyond the scope of this guide. Duffy and Arnold [17] as well as Duffy and Manderscheid [18] present reliability models for brittle composites, and have been incorporated into the research code C/CARES (Composite CARES).

The monolithic models highlighted here include the principle of independent action (PIA) model [19, 20], and Batdorf's model [21-25]. A general discussion is presented for each though a detailed development is omitted for the sake of brevity. In order to simplify the presentation of each model, recast equation 22 as

$$P_f = 1 - exp\left[-\int \psi \, dV \right] \quad \textbf{(25)}$$

where ψ is identified as a failure function per unit volume. What remains is the specification of the failure function ψ for each reliability model.

PIA – A Phenomenological Model

For the principle of independent action (PIA) model or the Barnett-Freudenthal approximation [19, 20], the failure function per unit volume is

$$\psi = \left(\frac{\sigma_1}{\sigma_0}\right)^m + \left(\frac{\sigma_2}{\sigma_0}\right)^m + \left(\frac{\sigma_3}{\sigma_0}\right)^m \quad \textbf{(26)}$$

where σ_1, σ_2 and σ_3 are the three principal stresses at a given point, and σ_0 is the Weibull material scale parameter. The PIA model is the probabilistic equivalent to the deterministic maximum stress failure theory. In this approach, the principal stresses are assumed to act independently in each principal direction. Failure probability is calculated from the product of the individual survival probabilities, in the direction of the tensile components. The PIA model has been widely applied in brittle material design; however, it does not specify the nature of the defect causing failure and has consequently been criticized by several authors because it ignores interaction of principal stresses and underestimates failure probabilities [23]. In essence, the model is phenomenological, which does not imply that the model is not useful; rather, the simplicity of a phenomenological model can often be a strength and not a weakness.

Batdorf's Theory - Mechanistic Model

The concepts proposed by Batdorf [21-25] are important in that the approach incorporates a mechanistic basis for the effect of multiaxial states of stress into the weakest-link theory. Here material defects distributed throughout the volume (and/or over the surface and/or along edges) are assumed to have a random orientation. In addition, the defects are assumed to be non-interacting discontinuities (cracks) with an assumed regular geometry. Consider a finite volume of material where the stress state is uniform throughout. Batdorf postulated that the probability of failure for this finite volume could be expressed by the following joint probability

$$P_f(\Sigma, \sigma_{cr}, \Delta V) = P_1 \, P_2 \quad \textbf{(27)}$$

Here Σ represents the uniform multiaxial state of stress throughout the finite volume. In addition, P_1 is the probability that a crack exists in ΔV (the finite volume) with an associated critical stress (i.e., fracture stress) in the range of σ_{cr} to $\sigma_{cr}+d\sigma_{cr}$. Note that σ_{cr} is defined as the critical far field normal stress for a given crack configuration under Mode I loading. The second marginal probability, P_2, denotes the probability that a crack with an associated critical stress of σ_{cr} will be oriented in a direction such that the effective far field applied stress, σ_e, equals or exceeds σ_{cr}. These two probabilities can be expressed as

$$P_1 = \Delta V \frac{d\eta(\sigma_{cr})}{\sigma_{cr}} d\sigma_{cr} \quad \textbf{(28)}$$

and

$$P_2 = \frac{\Omega}{4\pi} \quad \textbf{(29)}$$

The function $\eta(\sigma_{cr})$ is referred to as the Batdorf crack density function. This function is independent of the multiaxial stress state Σ. Typically the function is expressed in a power law format, i.e.,

$$\eta(\sigma_{cr}) = k_B (\sigma_{cr})^m \quad \textbf{(30)}$$

where m is the Weibull modulus and k_B is a material parameter, both of which can be estimated or computed from failure data.

In equation 29 the solid angle Ω is mapped onto a unit sphere in the principal stress space and represents all crack orientations for which

$$\sigma_e \geq \sigma_{cr} \quad \textbf{(31)}$$

Failure is assumed to occur when a far-field effective stress σ_e associated with the weakest flaw reaches a critical level, σ_{cr}. The effective stress σ_e is a predefined combination of the far field normal stress and the far field shear stress. It is also a function of the assumed crack configuration, the existing stress state, and the fracture criterion employed (hence the claim that the approach captures the physics of fracture). Accounting for the presence of a far-field shear stress reduces the far-field normal stress needed for fracture for special variations of the Batdorf model. The Batdorf model is defined by taking

$$P_f = 1 - exp\left[-\int_V \left[\int_0^{(\sigma_e)_{max}} \frac{\Omega}{4\pi} \frac{d\eta(\sigma_{cr})}{\sigma_{cr}} d\sigma_{cr} \right] dV \right] \quad \textbf{(32)}$$

Substituting for $\eta(\sigma_{cr})$ yields

$$P_f = 1 - exp\left[-\int_V \left[mk_B \int_0^{(\sigma_e)_{max}} \frac{\Omega}{4\pi} \sigma_{cr}^{m-1} d\sigma_{cr} \right] dV \right] \quad \textbf{(33)}$$

thus

$$\psi = mk_B \int_0^{(\sigma_e)_{max}} \frac{\Omega(\Sigma,\sigma_{cr})}{4\pi} \sigma_{cr}^{m-1} d\sigma_{cr} \quad \textbf{(34)}$$

for Batdorf's model.

The solid angle Ω is defined by the following expression

$$\Omega = \int_{\beta=0}^{2\pi} \int_{\alpha=0}^{\pi} H(\sigma_e, \sigma_{cr}) \sin\alpha \, d\alpha \, d\beta \quad (35)$$

where α and β are azimuthal angles in the principal stress space, and the Heaviside step function equals one, i.e.,

$$H(\sigma_e, \sigma_{cr}) = 1 \quad (36)$$

if

$$\sigma_e \geq \sigma_{cr} \quad (37)$$

The Heaviside step function in equation 35 is zero, i.e.,

$$H(\sigma_e, \sigma_{cr}) = 0 \quad (38)$$

if

$$\sigma_e < \sigma_{cr} \quad (39)$$

Inserting equations 34 and 35 into equation 33 leads to the following expression for the component probability of failure

$$P_f = 1 - exp\left[-\frac{k_{BV}}{2\pi} \int_V \int_{\beta=0}^{2\pi} \int_{\alpha=0}^{\frac{\pi}{2}} \left[\sigma_e(x,y,z,\alpha,\beta)\right]^{m_v} \sin\alpha \; d\alpha \; d\beta \; dV \right] \quad (40)$$

An alternative expression for component failure probability can be derived from equations 33 through 36 by utilizing notation advocated by Johnson and Tucker [26]. Here a stress gradient factor (I_V) is identified as

$$I_V = \left(\frac{k_{BV}}{2\pi}\right)\left(\frac{\sigma_0}{\sigma_{max}}\right)^{m_v}\left(\frac{1}{V}\right) \int_V \int_{\beta=0}^{2\pi} \int_{\alpha=0}^{\frac{\pi}{2}} {\sigma_e}^{m_v} \sin\alpha \, d\alpha \, d\beta \, dV \quad (41)$$

Now

$$P_f = 1 - exp\left[-I_V \; V \left(\frac{\sigma_{max}}{\sigma_0} \right)^{m_v} \right] \quad (42)$$

These expressions assume that flaws are distributed uniformly throughout the volume of the component. A similar development would lead to the following expression for failure due to flaws spatially distributed along the surface of the component (and analogously along edges), i.e.,

$$P_f = 1 - exp\left[-\frac{k_{BA}}{\pi} \int_A \int_0^{\pi} \left[\sigma_e(x,y,\alpha)\right]^{m_A} sin\alpha \; d\alpha \; dA \right] \quad (43)$$

Once again a stress gradient factor associated with a surface area analysis (I_A) can be introduced, i.e.,

$$I_A = \left(\frac{k_{BA}}{2\pi} \right) \left(\frac{\sigma_0}{\sigma_{max}} \right)^{m_A} \left(\frac{1}{A} \right) \int_A \int_0^{\pi} {\sigma_e}^{m_A} sin\alpha \; d\alpha \; dA \quad (44)$$

Then

$$P_f = 1 - exp\left[-I_A \; A \left(\frac{\sigma_{max}}{\sigma_0} \right)^{m_A} \right] \quad (45)$$

The crack density coefficient k_B that appears in the expressions above is obtained from failure data. There is a theoretical development that appears in the WeibPar Users Manual that outlines the methodology for obtaining estimates of the Weibull parameters m and σ_0. Once these quantities are estimated k_B can be computed since

$$k_B = k_B(m, \sigma_\theta, SpecimenGeometry) \quad (46)$$

The parameter k_B is a material specific parameter in much the same manner that σ_0 (the Weibull material scale parameter) is a material specific parameter. The specimen geometry incorporated in the expression above is compensated by the fact that σ_θ is also dependent on specimen geometry. Thus the form of the expression above changes from specimen type, but the estimated value of σ_θ will also change, and the result is that the computed value of the crack density coefficient should stay consistent from test geometry to test geometry for a given material. In addition, the Weibull material scale parameter σ_0 is also a function of m, σ_θ, and the specimen geometry, i.e.,

$$\sigma_0 = \sigma_0(m, \sigma_\theta, SpecimenGeometry) \quad (47)$$

Expressions for σ_0 associated with several simple bend geometries can be found in ASTM C1239 [15].

Numerous authors have discussed the stress distribution around cavities of various types, under different loading conditions, and proposed numerous criteria to describe impending fracture. A good compendium of fracture based reliability models can be found in Nemeth, *et al.* [27]. However, several issues must be pointed out. No prevailing consensus has emerged regarding a best probabilistic fracture theory. Most current models predict somewhat similar reliability results, despite the divergence of initial assumptions. Moreover, one must approach the mechanistic models with some caution. For example, the reliability models based on fracture mechanics incorporate the assumptions made in developing the fracture models on which they are based. One of the fundamental assumptions made in the derivation of fracture mechanics criteria is that the crack length is much larger than the characteristic length of the microstructure. This is sometimes referred to as the continuum principle in engineering mechanics. For ceramic materials that characteristic length is the grain size (or diameter). If one contemplates the fact that most ceramic materials are high strength with attending low fracture toughness, then the critical defect size can be quite small. If the critical defect size approaches the grain size of the material, then the Batdorf models discussed above should be based on the physics of cleavage fracture through or around single crystal microstructures.

LIFE PREDICTION (TIME-DEPENDENT)

The ability of a brittle material component to sustain load degrades over time due to a variety of effects such as oxidation, creep, thermo-chemical erosion, stress corrosion, and fatigue. Available time-dependent probabilistic component design involves predicting the probability of failure for a thermo-mechanically loaded component based on specimen rupture data. Typically experiments are performed using simple specimen geometries, i.e., flexural or tensile test specimens. A static (creep), monotonically increasing, or dynamic (cyclic) load is applied to a specimen until fracture occurs in a brittle fashion. The methods outlined in this section combine the statistical nature of strength-controlling flaws presented earlier with the mechanics of crack growth to capture the effects of multiaxial stress states, concurrent (simultaneously occurring) flaw populations, and scaling effects. Using these statistical parameters along with a multiaxial time-dependent reliability model, as well as the results obtained from a finite element analysis, an engineer can predict the life of a component. This is accomplished by generating the component's reliability as a function of time. When the component reliability falls below a predetermined reliability value, the associated point in time at which this occurs is assigned the life of the component.

Subcritical Crack Growth (SCG)

With load histories at stress levels that do not induce fast fracture, there is a regime defined by load and temperature where SCG occurs. Models for SCG that have been developed tend to be semi-empirical and approximate the behavior of crack growth phenomenologically. Experimental data indicates that crack growth rate (*da/dt*) is a function of the applied stress intensity factor, K_I (or the range in the stress intensity factor), such as illustrated in Figure 3. Curves of experimental data show three distinct regimes of growth when the data is graphically depicted as the logarithm of the rate of crack growth versus the logarithm of the Mode I stress intensity factor. The first region indicates threshold behavior of the crack, where below a certain value of stress intensity (K_{th}) crack growth is zero. The second region shows an approximately linear relationship of stable crack growth. The third region indicates unstable crack growth as the material's critical stress intensity factor (K_{1C}) is approached. The second region typically dominates the life of the material. For the stress corrosion failure mechanism, these curves are material and environment sensitive.

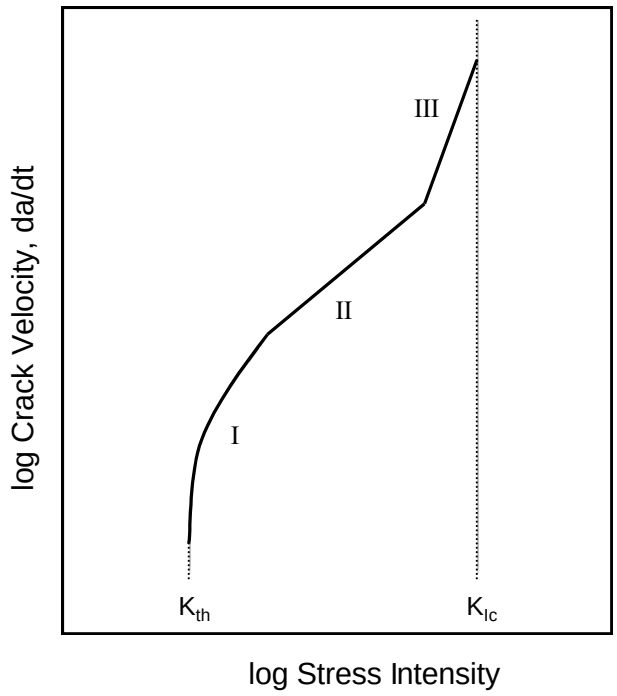

Figure 3 Crack Velocity as a Function of Stress Intensity (K) in Monolithic Ceramics. Crack Initiation Does Not Occur when $K<K_{th}$. SCG can occur when $K_{th}<K<K_{Ic}$ (Regions I, II, and III). Fracture occurs when $K> K_{Ic}$.

The SCG models cited most often in the literature are based on power law formulations for the rate equations. Power law formulations are used to model the second region of the experimental data cited above. This power law formulation is expressed as

$$\frac{da(x,y,z,t)}{dt} = A K_{Ieq}^{N}(x,y,z,t) \quad \textbf{(48)}$$

where *A* and *N* (crack growth exponent) are material/environmental constants. Utilizing the following classical fracture mechanics expression

$$K_{Ieq}(x,y,z,t) = \sigma_{Ieq}(x,y,z,t) Y \sqrt{a(x,y,z,t)} \quad \textbf{(49)}$$

by inserting it into equation 48 leads to

$$\frac{da(x,y,z,t)}{dt} = A \left(\sigma_{Ieq}\right)^{N}(x,y,z,t) \; Y^{N} \; a^{N/2}(x,y,z,t) \quad \textbf{(50)}$$

where *Y* is a function of crack geometry, and *a(x,y,z,t)* represents the crack length at time *t*. Separation of variables leads to the following integral

$$\int_{t=0}^{t_f} \left(\sigma_{Ieq}\right)^{N} dt = \left(\frac{1}{AY^{N}}\right) \int_{a=a_o}^{a_f} a^{-N/2} da \quad \textbf{(51)}$$

Note that from equation 49 the initial critical flaw size can be expressed

$$a_0 = \left(\frac{K_{Ieq,C}}{\sigma_{Ieq,0}\, Y} \right)^2 \quad \textbf{(52)}$$

and the critical flaw size at failure can be expressed

$$a_f = \left(\frac{K_{Ieq,C}}{\sigma_{Ieq,f}\, Y} \right)^2 \quad \textbf{(53)}$$

Since component failure is the primary concern as the critical flaw grows from a_0 to a_f, then the stress intensity factors appearing in equations 52 and 53 are critical stress intensities. These expressions for the flaw lengths a_0 and a_f are substituted for the limits appearing in equation 51. Integration of equation 51 yields the following expression

$$\sigma_{Ieq,0}(x,y,z,t_f) = \left[\frac{\int_0^{t_f} \sigma_{Ieq}^N(x,y,z,t)\,dt}{B} + \sigma_{Ieq,f}^{N-2}(x,y,z,t_f) \right]^{\frac{1}{(N-2)}} \quad \textbf{(54)}$$

Equation 54 provides the basis for computing time-dependent reliability. In this equation $\sigma_{Ieq,0}$ represents the equivalent applied far field stress that will fail a critical flaw with an initial length of a_0 under a fast fracture load rate. This far field stress is equal to the right hand side of equation 54 which is comprised of a load history that will produce failure when the critical flaw has grown to a length a_f. Since

$$a_0 < a_f \quad \textbf{(55)}$$

then

$$\sigma_{Ieq,0} > \sigma_{Ieq,f} \quad \textbf{(56)}$$

and the integral expression appearing in equation 54 is necessary for equality to hold. The integral expression represents the process of growing the critical flaw from a_0 to a_f in a subcritical fashion. If the right hand side of equation 54 can be evaluated, either in closed form or numerically, then the probability of failure at time t_f can be computed using fast fracture expressions along with the value of $\sigma_{Ieq,0}$. This is the computational approach adopted in the CARES/Life and allows the design engineer to evaluate time-dependent reliability. Using the PIA model or the Batdorf theory accommodates multiaxial stress fields. These multiaxial reliability expressions were outlined in previous sections for time-independent reliability analysis models. For the sake of brevity in this chapter we will focus on development of the SCG reliability model utilizing the Batdorf theory. Note that in equation 54

$$B = \frac{2}{AY^2 K_{Ieq,C}^{N-2}(N-2)} \tag{57}$$

The parameter B has units of *stress*^{2} *x time*. The crack geometry factor Y is assumed constant for subcritical crack growth. The parameters A, Y and K_{Ic} are never computed directly, but are manifested through the parameter B via the expression above, and a value for the parameter B is estimated from experimental data.

Time-Dependent Batdorf Model

The determination of the time dependent component probability of failure using the Batdorf model parallels that presented earlier for fast fracture. Equation 54 is modified by taking

$$\begin{aligned} \sigma_e &= \sigma_{Ieq,0}(x,y,z,t_f) \\ &= \left[\frac{\int_0^{t_f} \sigma_{Ieq}^N(x,y,z,t)\,dt}{B} + \sigma_{Ieq,f}^{N-2}(x,y,z,t_f) \right]^{\frac{1}{(N-2)}} \end{aligned} \tag{58}$$

Substitution of this expression for σ_e into equation 39 yields

$$P_f = 1 - exp\left[-\frac{k_{BV}}{2\pi} \int_V \int_0^{2\pi} \int_0^{\frac{\pi}{2}} \left[\sigma_{Ieq,0}(x,y,z,t_f)\right]^{m_v} \sin\alpha \, d\alpha \, d\beta \, dV \right] \tag{59}$$

A similar substitution into equation 43 yields

$$P_f = 1 - exp\left[-\frac{k_{BA}}{\pi} \int_A \int_0^{\pi} \left[\sigma_{Ieq,0}(x,y,t_f)\right]^{m_v} \sin\alpha \, d\alpha \, dA \right] \tag{60}$$

The transformed equivalent stress $\sigma_{Ieq,0}$ is dependent on the load history, the selected fracture criterion, crack shape, and time to failure, t_f. The formulation of $\sigma_{Ieq,0}$ for creep and monotonically increasing load histories are presented below because closed form expressions can be derived. A similar development exists for the PIA model. For the sake of brevity it is omitted from this discussion. Expressions for cyclic fatigue are available (e.g., Mencik [28]).

Static Fatigue

Static fatigue is defined by the engineer as time-dependent strength degradation under a constant load. Integrating the right hand side of equation 58 with respect to time yields (assuming constant stress)

$$\sigma_{Ieq,0}(x,y,z) = \sigma_{Ieq,f}(x,y,z,t=t_f) \left[\frac{t_f \sigma_{Ieq,f}^2(x,y,z,t=t_f)}{B} + 1 \right]^{\frac{1}{N-2}} \tag{61}$$

Dynamic Fatigue

Monotonically increasing uniaxial loading, referred to as dynamic fatigue, is defined as the application of a constant stress rate $\dot{\sigma}(x, y, z)$ over a period of time, *t*. Dynamic fatigue is an established [29], effective and valid accelerated static fatigue test (see Figure 4) to determine slow crack growth parameters if and only if the same dominant fatigue-limiting mechanism is operative under static and dynamic loadings. Assuming the applied stress is zero at time *t=0*, then

$$\begin{aligned} \sigma_{Ieq}(x,y,z,t) &= \sigma(t) \\ &= t\,\dot{\sigma}(x,y,z) \end{aligned} \qquad \textbf{(62)}$$

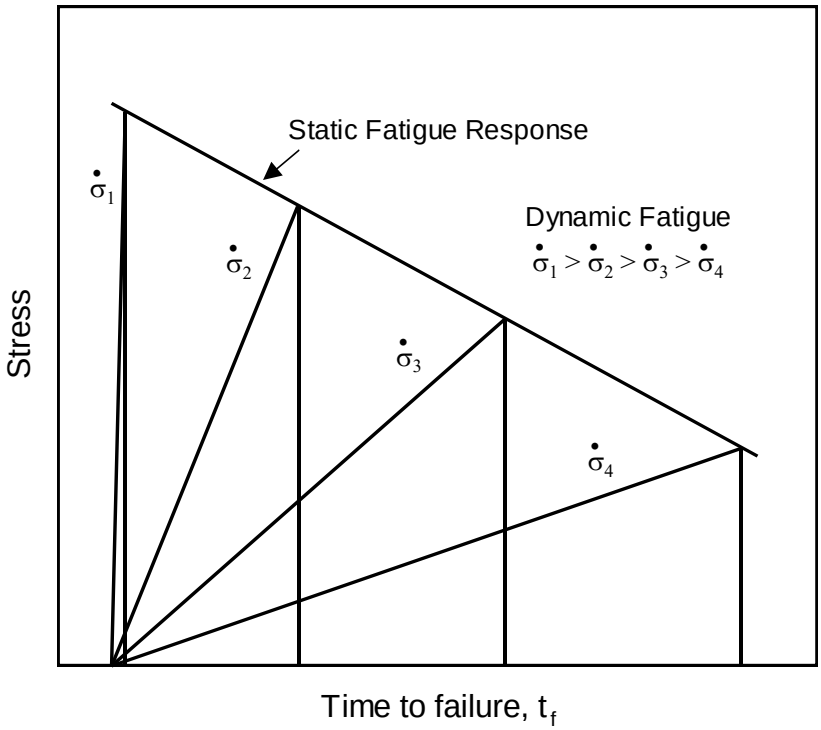

Figure 4 Dynamic Fatigue Testing is an Effective Accelerated Test for Static Fatigue Response if the Same Dominant Fatigue Mechanism is Operative.

Substituting equation 61 into equation 58 results in the following expression for effective stress

$$\sigma_{Ieq,0}(x,y,z) = \left\{\left[\frac{1}{\dot{\sigma}(N+1)B}\right]\sigma_{Ieq,f}^{N+1}(x,y,z,t=t_f) + \sigma_{Ieq,f}^{N-2}(x,y,z,t=t_f)\right\}^{\frac{1}{N-2}} \qquad \textbf{(63)}$$

Note that only several load histories have been discussed above. These load histories correspond to analyses with closed form solutions. Several other load histories associated with cyclic fatigue have closed form solutions. These solutions are omitted for the sake of brevity.

REFERENCES

1. Richerson, D. W. and Anson, D., "Evolution of Ceramic Gas Turbine Development Programs at Engine Manufacturers in the United States," Chapter 2 in *Ceramic Gas Turbine Design and Test Experience, Progress in Ceramic Gas Turbine Development, Volume 1,* M. van Roode, M. K. Ferber, and D. W. Richerson, eds., ASME Press, New York, NY, USA, 2002. pp. 11-16.
2. Hartsock, D. L., "Ford's Development of the 820 High Temperature Ceramic Gas Turbine Engine," ibid., Chapter 3, pp. 17-75.
3. Morrison, J., Lane, J., and Burke, M., "Progress in Ceramic Gas Turbine Development Westinghouse/Siemens Westinghouse," ibid., Chapter 8, pp. 193-223.
4. Khandelwal, P. and Heitman, P, "Ceramic Gas Turbine Development at Rolls-Royce in Indianapolis," ibid., Chapter 5, pp. 111-132.
5. Schenk, B., Easley, M. L., and Richerson, D. W., "Evolution of Ceramic Turbine Engine Technology at Honeywell Engines, Systems & Services," ibid., Chapter 4, pp. 77-109.
6. Powers, L. M. and Janosik, L. A., "A Numerical Round Robin for the Reliability Prediction of Structural Ceramics," AIAA Paper 93-1498, in *34th AIAA/ASME/ASCE/AHS/ASC Structures, Structural Dynamics, and Materials Conference,* AIAA/ASME Adaptive Structures Forum, La Jolla, CA, USA, Apr. 19-22, 1993, Technical Papers, Pt. 3 (A93-33876 13-39), 1993. pp. 1647-1658.
7. Dortmans, L., Thiemeier, T., and Brückner-Foit, A., "WELFEP: A Round Robin for Weakest-Link Finite Element Postprocessors," Journal of the European Ceramic Society, 11,17-22, 1993
8. Bornemisza, T. and Jones, A., "Ceramic Gas Turbine Development at Hamilton Sundstrand Power Systems," Chapter 6 in *Ceramic Gas Turbine Design and Test Experience, Progress in Ceramic Gas Turbine Development, Volume 1,* M. van Roode, M. K. Ferber, and D. W. Richerson, eds., ASME Press, New York, NY, USA, 2002. pp. 133-154.
9. Brentnall, W. D., van Roode, M., Norton, P. F., Gates, S., Price, J. R., Jimenez, O., and Miriyala, O., "Ceramic Gas Turbine Development at Solar Turbines Incorporated," ibid., Chapter 7, pp. 155-192.
10. Itoh, T. and Sugawara, A., "Evolution of Ceramic Gas Turbine Development Programs at Engine Manufacturers in Japan," ibid., Chapter 12, pp. 277-281
11. van Roode, M., "Evolution of Ceramic Gas Turbine Development Programs at Engine Manufacturers in Western Europe," ibid., Chapter 20, pp. 445-452.
12. Wereszczak, A. A., Kirkland, T. P., Breder, K., Lin, H. -T., and Andrews, M. J., "Biaxial Strength, Strength-Size-Scaling, and Fatigue Resistance of Alumina and Aluminum Nitride Substrates," International Journal of Microcircuits and Elect. Packaging, 22, 446-458, 1999.
13. Weibull, W.A., "The Phenomenon of Rupture in Solids," Ingeniors Vetenskaps Akademien Handlinger, No. 153, 1939.
14. Weibull, W. A., "A Statistical Distribution Function of Wide Applicability," Journal of Applied Mechanics, 18[3], 293–297, 1951.
15. "Practice for Reporting Uniaxial Strength Data and Estimating Weibull Distribution Parameters for Advanced Ceramics," ASTM C1239, Vol. 15.01, Annual Book of ASTM Standards, American Society for Testing and Materials, Conshohocken, PA, USA, 2002.

16. "Standard Practice for Fractography and Characterization of Fracture Origins in Advanced Ceramics," ASTM C1322, Vol. 15.01, Annual Book of ASTM Standards, American Society for Testing and Materials, Conshohocken, PA, USA, 2002.
17. Duffy, S. F. and Arnold, S. M., "Noninteractive Macroscopic Statistical Failure Theory for Whisker Reinforced Ceramic Composites," Journal of Composite Materials, 24[3], 293-308, 1990.
18. Duffy, S. F. and Manderscheid, J. M., "Noninteractive Macroscopic Reliability Model for Ceramic Matrix Composites with Orthotropic Material Symmetry," Transactions of the ASME, Journal of Engineering for Gas Turbines and Power, 112[4], 507-511, 1990.
19. Barnett, R. L., Connors, C. L., Hermann, P. C., and Wingfield, J. R., *Fracture of Brittle Materials Under Transient Mechanical and Thermal Loading*, U.S. Air Force Flight Dynamics Laboratory, AFFDL-TR-66-220, March, 1967.
20. Freudenthal, A. M., "Statistical Approach to Brittle Fracture. Fracture, An Advanced Treatise," in *Mathematical Fundamentals, Vol. 2,* H. Liebowitz, ed., Academic Press, New York, NY, USA, 1968. pp. 591-619.
21. Batdorf, S. B. and Crose, J. G., "A Statistical Theory for the Fracture of Brittle Structures Subjected to Nonuniform Polyaxial Stresses," Journal of Applied Mechanics, 41[2], 459-464, 1974.
22. Batdorf, S. B., "Weibull Statistics for Polyaxial Stress States," Journal of the American Ceramic Society, 57[1], 44-45, 1974.
23. Batdorf, S. B., "Some Approximate Treatments of Fracture Statistics for Polyaxial Tension," International Journal of Fracture, 13, 5-11, 1977.
24. Batdorf, S. B., "Fundamentals of the Statistical Theory of Fracture," pp. 1-30 in *Fracture Mechanics of Ceramics, Vol. 3,* Bradt, R. C., Hasselman, D. P. H. and Lange, F. F., eds., Plenum Press, New York, NY, USA, 1978.
25. Batdorf, S. B. and Heinisch, H. L., "Weakest Link Theory Reformulated for Arbitrary Fracture Criterion," Journal of the American Ceramic Society, 61[7-8], 355-358, 1978.
26. Johnson, C. A. and Tucker, W. T., "Derivation of Statistical Models," in *Life Prediction Methodology for Ceramic Components of Advanced Heat Engines – Phase I Final Report*, Volume I, Contract No. 86X-SC674C, 1994. pp. 5-60.
27. Nemeth, N. N., Manderscheid, J. M., and Gyekenyesi, J. P., *Ceramics Analysis and Reliability Evaluation of Structures (CARES) Users and Programmers Manual*, NASA TP-2916, 1990.
28. Mencik, J., "Rationalized Load and Lifetime of Brittle Materials," Communications of The American Ceramic Society, 67, 110-116, 1984.
29. "Test Method for Determination of Slow Crack Growth Parameters of Advanced Ceramics by Constant Stress-Rate Flexural Testing at Ambient Temperature," ASTM C1368, Vol. 15.01, Annual Book of ASTM Standards, American Society for Testing and Materials, Conshohocken, PA, USA, 2002.